MIR-467 PREVENTS INFLAMMATION AND INSULIN RESISTANCE IN RESPONSE TO HYPERGLYCEMIA

Jasmine Gajeton[1,2], Irene Krukovets[1], Revanth Yendamuri[1], Dmitriy Verbovetskiy[1], Amit Vasanji[3], Lidiya Sul[1], Olga Stenina-Adognravi[1,2]

[1]Department of Cardiovascular & Metabolic Sciences, Cleveland Clinic, Cleveland, OH, USA

[2]Department of Molecular Medicine, Case Western Reserve University, Cleveland, OH, USA

[3]ERT Imaging, Cleveland, OH, USA

Address correspondence to:

Olga Stenina-Adognravi

Department of Molecular Cardiology, Cleveland Clinic

9500 Euclid Ave NB50-78, Cleveland, OH 44195

(216) 444-9057

stenino@ccf.org

Word count: 3,954

ABSTRACT

Poor diets and obesity are associated with inflammation and insulin resistance (IR), but the physiological regulation of insulin sensitivity (IS) is not completely understood. We report that miR-467, induced by elevated blood glucose levels, decreases inflammation and IR in a diet-induced IR model. In Western diet-fed mice, miR-467 antagonist injections increased IR compared to mice injected with a control oligonucleotide. In mice injected with the antagonist, we detected elevated blood glucose (143 vs 121.7 mg/dL); higher plasma insulin levels (98 vs 63 ng/mL); lower insulin sensitivity; increased adipocyte size; and increased recruitment of macrophages into adipose tissue and pancreas (by 47% in adipose tissue; 44% in pancreas), without increases in weight or lipoproteins and cholesterol levels.

Lack of miR-467 antagonist effects in *Thbs1*$^{-/-}$ mice (deficient in thrombospondin-1, TSP-1, a target of miR-467 that we have experimentally confirmed elsewhere) in response to the miR-467 antagonist suggested that TSP-1 mediates some effects of miR-467 in preventing IR. Not all effects by the miR-467 antagonist were abolished in Thbs1$^{-/-}$ mice and their macrophages, suggesting that miR-467 employs multiple targets in regulating inflammation and IR.

Our results demonstrate that miR-467 provides a physiological feedback to prevent inflammation and IR in response to dietary signals.

INTRODUCTION

Diet-induced obesity correlates with inflammation and IR (1). However, the sequence and the causality of the pathological changes leading to the IR are still poorly understood.

Studies in *Thbs1*$^{-/-}$ mice suggest that a lack of TSP-1 may alleviate chronic inflammation and IR associated with obesity (2-4). Macrophage-specific deletion of *Thbs1*$^{-/-}$ alone was sufficient to protect the animals from IR (2).

We recently reported that miR-467 is rapidly upregulated by hyperglycemia in endothelial cells (EC) and regulates cancer angiogenesis by targeting TSP-1 mRNA (5; 6). Others reported that this miRNA prevented vascular inflammation and atherosclerosis development by targeting Lipoprotein Lipase in macrophages (7; 8). However, the physiological function of this miRNA and the physiological significance of its rapid upregulation by hyperglycemia remained unknown.

In this work, we employed a diet-induced IR model to examine the effects of miR-467 inhibition on IR. Mice received the weekly systemic injections of a sequence-specific miR-467 antagonist. The effects of the antagonist on glucose and insulin levels, insulin sensitivity, and inflammation in adipose tissue and pancreas were examined in wild type mice (WT) and *Thbs1*$^{-/-}$ mice to understand the role of miR-467 and its target TSP-1 in regulation of inflammation in tissues and in the development of IR.

RESEARCH DESIGN AND METHODS

Experimental animals

Animal procedures were approved by the Institutional Animal Care and Use Committee. Mice were fed a chow or Western diet (TD.88137, 40-45% kcal from fat, 34% sucrose by weight, Envigo) starting at 4 weeks of age and injected weekly with a miR-467 antagonist (2.5 mg/kg body weight), intraperitoneally, starting at 5 weeks of age until the end of the experiment.

miR-467 mimic and the miR-467 antagonist

The miR-467 mimic and the control oligonucleotide were purchased from Dharmacon. Cholesterol conjugated miR-467 was modified by tagging of the fluorophore DY547 and a cholesterol moiety. The custom LNA-modified miR-467 antagonist (TacaTGcaGGcacTTa) and a control oligonucleotide (TTTaGaccgaGcgTGt) were from Qiagen.

Glucose and insulin tolerance tests (GTT and ITT)

GTT and ITT were administered after overnight fasting. Glucose (2 g/kg body weight) or insulin (50 mg/kg) (Sigma) were injected intraperitoneally. Blood glucose levels were measured 0 - 180 min after the injection using an AlphaTRAK glucometer.

Induction of diabetes in mice

Mice were given IP streptozotocin (STZ, Sigma) injections (50 mg/kg) for 5 consecutive days. Mice with blood glucose >250 mg/dL were selected for experiments.

Blood cell counts, lipoprotein profile, and cytokines in blood

Blood was collected by cardiac puncture, and circulating blood cell counts were analyzed using an ADVIA 120 Hematology System (Siemens). Plasma insulin was measured using an Insulin Mouse ELISA kit (Thermo).

A custom U-plex Assay Platform (MSD) was used to assess plasma levels of IL-1β, IL-2, IL-4, IL-6, IL-10, KC, MCP-1, MIP-1β, TNF-α, and VEGF-A.

Lipoproteins were measured using the HDL and LDL/VLDL quantification kit (BioVision) at end of the experiment.

Immunohistochemical staining

Adipose tissue and pancreas were fixed in 4% formaldehyde (Electron Microscopy Sciences) for 24 hours, then transferred into 70% ethyl alcohol and embedded in paraffin blocks. 5 μM sections of tissues were stained with Hematoxylin (Ricca), Eosin (Protocol), Masson's trichrome, or specific antibodies using Vecta Stain ABC Kit (Vector Labs).

Adipocyte sizes were quantified in H&E stained sections by ERT Imaging (Cleveland, OH).

Sections were stained with anti-CD68 (AbD Serotec), anti-Insulin (Dako), MOMA-2 (AbD Serotec), anti-vWF (Dako), anti-α-actin (Abcam), or ati-TSP-1 Ab4 (Thermo). Slides were scanned using Leica SCN400 or Aperio AT2 at 20X magnification. Positive staining in the images was quantified using Photoshop CS2 (Adobe) or Image Pro Plus (7.0).

Cell culture

RAW264.7, THP-1, βTC6 and 3T3-L1 cells were purchased from ATCC and cultured according to ATCC directions. THP-1 cells were differentiated in 100 nM PMA (Sigma) for 3 days before glucose stimulation. 3T3-L1 cells were differentiated at 80% confluency with 1μM Dexamethasone, 0.5 mM IBMX, and 1 μg/mL Insulin (all from Sigma).

Isolation of bone marrow-derived macrophages (BMDM)

Bone marrow was collected from femurs and tibia as described in (9). Macrophages were differentiated from whole bone marrow using 30 ng/mL MCSF (Biolegend) for 4 days, followed by 15 ng/mL MCSF for 3 days.

Glucose stimulation of RAW264.7, differentiated THP-1, βTC6, and BMDM

Up to 1.0 x10^6 cells were plated in complete media in 6-well plates (Corning). Once glucose levels reached the fasting level (90 mg/dL) as measured using AlphaTRAK glucometer, cells were stimulated with 30 mM D-glucose High Glucose, “HG” (Sigma) for 6 hours (RAW 264.7 and BMDM), 3 hours (3T3-L1) or 30 minutes (βTC6).

Transfection of cultured cells

Transfection of the miR-467 antagonist and its control oligo were aided with Oligofectamine (Invitrogen) for 24 hours. Successful transfection with the cholesterol-modified miR-467 mimic was confirmed by fluorescence 24 hours post-transfection using an inverted microscope DMI6000SD (Leica).

Oil Red O Staining

Differentiated 3T3-L1 cells were washed with 1X PBS and fixed in 10% formalin (Electron Microscopy Sciences) for 15' at room temperature (RT), washed with 60% isopropanol (Sigma) , and stained in the Oil Red O solution for 10' at RT.

RNA Extraction and QRT-PCR

RNA was isolated using Trizol reagent (Thermo). Organs were flash frozen in liquid nitrogen and homogenized in Trizol. RNA was quantified using Nanodrop 2000 (Thermo).

To measure miR-467 expression, 1 – 2.5 μg of total RNA was first polyadenylated using NCode miRNA First-Strand cDNA Synthesis kit (Invitrogen) or miRNA 1st strand cDNA synthesis kit (Agilent). Real-time PCR amplification was performed using SYBR GreenER™ qPCR SuperMix Universal (Thermo) or miRNA QPCR Master Mix (Agilent). The miR-467 primer (GTA AGT GCC TAT GTA TATG) was purchased from IDT.

To measure expression of inflammatory markers, 1 – 2 μg of total RNA was used to synthesize cDNA using the SuperScript First-Strand cDNA Synthesis System for RT-PCR (Invitrogen). Real-time PCR was performed using TaqMan primers for TNFA, IL6, CCL2, IL1B, IL10, CCL4 (Thermo) and TaqMan Fast Advanced Master Mix (Thermo).

Statistical analysis

Data are expressed as the mean value ± SD (standard deviation). Statistical analysis was performed using GraphPad Prism 5 Software. A p-value of <0.05 was considered statistically significant.

RESULTS

Systemic injections of miR-467 antagonist increase fasting blood glucose and insulin levels in mice

Four-week-old male C57BL/6 WT mice on chow or Western diets were injected with a miR-467 antagonist (2.5 mg/kg) weekly for 32 weeks, starting at 5 weeks of age. At the end of the experiment, fasting blood glucose and insulin levels were measured. As expected, both blood glucose and insulin levels were significantly increased in Western diet-fed mice (Fig. 1*A* and *B*). Injections of the antagonist resulted in further increase of blood glucose levels in mice on the Western diet (Fig. 1*A*) and increased blood insulin levels in chow-fed mice to levels identical to those of mice on the Western diet (Fig. 1*B*).

Systemic injections of miR-467 antagonist decrease insulin sensitivity

Glucose and insulin tolerance tests were performed at the end of the experiment.

miR-467 antagonist injections caused higher levels of blood glucose in mice on Western diet 60 – 120 min after the glucose injections in GTT (Fig. 1*C*). In the ITT, blood glucose levels were also higher at several time points after the injection of insulin in ITT (Fig. 1*D*). The Western diet decreased glucose tolerance (GTT area under curve increased from 2042.2 $\pm$ 333.7 in chow-fed mice to 2417 $\pm$ 402.6 in mice on Western diet, p=0.018, n=10) (Fig. 1*E*) and insulin sensitivity (ITT area under curve increased from 505.8 $\pm$ 51.52 in chow-fed mice to 549.8 $\pm$ 60.5 in mice on Western diet, p=0.048, n=10) (Fig. 1*F*).

The antagonist injections tended to decrease insulin sensitivity in both the chow and Western diet groups as compared to the injections of the control oligonucleotide. In mice on chow injected with the antagonist, ITT area under curve was 553.9 $\pm$ 119.6,

reaching the values similar to the Western diet group, versus 505.8 ± 51.52 in mice injected with the control oligonucleotide (p=0.13, n=10). In Western diet-fed mice, the antagonist increased the area under the curve to 623.5 ± 122.8 versus 549.8 ± 60.5 in mice on Western diet injected with the control oligonucleotide (p=0.05, n=10) (Fig. 1*F*).

Systemic injections of miR-467 antagonist do not affect the weight or lipid profile

The weight of Western diet-fed mice was significantly higher than in the chow-fed mice, as expected (Fig. 1*G*). However, the weight of the animals was not affected by the miR-467 antagonist injections on either diet.

To assess whether lipoprotein levels were affected by the miR-467 antagonist, serum was assayed for levels of high density lipoproteins (HDL), low density lipoproteins (LDL), and cholesterol as described in Methods. Both lipoproteins and cholesterol were significantly higher in mice on the Western diet, as expected (Fig. 1*H*). However, injections of the miR-467 antagonist did not affect the lipid profile on either diet.

Injections of miR-467 antagonist increase macrophage accumulation in adipose tissue

Macrophage accumulation in adipose tissue and pancreas was assessed by immunohistochemistry using an anti-MOMA-2 or anti-CD68 antibody followed by the quantification of the positively stained area (Fig. 2*A* and *B*, respectively).

Western diet-fed mice had significantly increased accumulation of macrophages in adipose tissue (Fig. 2*A*, p=0.0360). Injections of the miR-467 antagonist significantly increased macrophage accumulation in chow-fed mice (47% increase, p=0.0360), from 86.81%±5.514 to levels comparable to mice on the Western diet (128.5%±13.68). There

was no further increase in response to antagonist in mice on Western diet (146.3%±26.18, p=0.4698).

In the pancreas, accumulation of macrophages was also increased in mice on Western diet (73% increase, p=0.0172, Fig. 2*B*) from 1.00%±0.1106 in chow-fed mice to 1.73%±0.2194 in mice fed the Western diet. Injections of the miR-467 antagonist increased the accumulation of macrophages (44% increase, p=0.0436) in Western diet-fed mice from 1.73%±0.2194 to 2.50%±0.3607 with the antagonist. Injections of the miR-467 antagonist also increased the accumulation of macrophages in mice on the chow diet by 62% to 1.624%±0.4787, but it did not reach statistical significance (p=0.1224).

miR-467 antagonist has differential effects on the expression of inflammatory markers in adipose tissue

Expression of *Il6, Tnfa*, *Ccl2*, *Ccl4*, or *Il1b* was assessed by QRT-PCR in chow or Western diet-fed injected with the control oligonucleotide or the miR-467 antagonist (Fig. 3*C*).

Out of five cytokines, the levels of three, *Il6*,*Tnfa*, and *Ccl2*, were affected by the antagonist: *IL6* expression was upregulated by inhibition of miR-467 in mice on chow to levels similar to mice on the Western diet. *Tnfa* and *Ccl2* mRNA levels were decreased in response to the miR-467 antagonist in Western diet-fed mice (Fig. 3*C*). *Ccl4* and *Il1b* expression were not affected by the antagonist.

miR-467 antagonist does not change numbers of circulating monocytes or WBCs

White blood cells (WBC) and monocytes were counted in whole blood samples of mice on both diets injected with the control oligonucleotide or with miR-467 antagonist (Fig. 2*D-E*). There was no effect of the antagonist on the numbers of WBC or monocytes in blood in either WT or *Thbs1*$^{-/-}$ mice.

miR-467 in adipose tissue and the effects of the antagonist injections

Differentiated 3T3-L1 responded to glucose stimulation by increasing levels of miR-467 by 21.8%±13.81 (Fig. 3A, p=0.0203). However, at the end of the animal experiment, we did not find any differences in miR-467 levels in the adipose tissue of mice on the chow or Western diet (Fig. 3*B)*.

Adipocyte size (mean area and perimeter) was increased by the Western diet (control oligo-injected mice, mean area pixels 2967±474.2compared to 1720±284.6in chow diet, p< 0.0001; 467-antagonist injected mice, mean area pixels 3225±487.8 compared to 1847±331.6in chow-fed mice, p<0.0001; n=10/group). Adipocyte size tended to increase in mice on the diets in response to miR-467 antagonist injections (mean area pixels 1847±331.6 in antagonist injected chow diet compared to 1720±284.6 in chow control-injected mice, p=0.1976; 3225±487.8 in antagonist-injected Western diet compared to 2967±474.2in control injected mice, p=0.1288, n=10/group, Fig. 3*C* and *D*).

To assess how TSP-1 protein levels were changed in the adipose tissue, sections were stained with an anti-TSP-1 antibody and quantified for positive staining (Fig. 3*E*). Western diet caused decreased levels of TSP-1 in adipose tissue by 71.40% and 66.52% in control oligo injected and 467-antagonist injected mice, respectively (control oligo-injected: 2.264%±0.874 chow compared to 0.6476%±0.2434 in Western diet,

p=0.0006; 467-antagonist: 2.882%±1.147 compared to 0.9647%±0.4988 in Western diet, p=0.007). As expected, the antagonist tended to rescue TSP-1 levels by 27.30% and 48.97% compared to control oligo injected mice on chow or Western diet, respectively (2.882%±1.147 in chow, p=0.1678 compared to 0.9647%±0.4988 in Western diet, p=0.1588).

Fibrosis in the adipose tissue affects remodeling and growth of the adipocytes (10-12), thus, adipose tissue sections were stained with Masson's Trichrome to assess extracellular matrix content as a measure of tissue fibrosis (Fig. 3*F*). There was no difference in staining between the mouse groups.

High glucose upregulates miR-467 in macrophages

Murine macrophages (RAW 264.7) and differentiated human monocyte (THP-1) cell lines were stimulated with high glucose (HG, 30mM D-glucose), and the levels of miR-467 were measured. miR-467 was upregulated by 20.6%±14.31 or 540.3%± 559.5 in response to hyperglycemia (Figs. 4*A* and *C*, respectively). Increased miR-467 levels were associated with a decrease in TSP-1 production by the cells (Fig. 4*B* and *D,* respectively, *p<0.05). Consistent with the mechanisms of miR-467 upregulation by high glucose described by us earlier (5; 13), both D-glucose and L-glucose had similar effect, indicating the osmolarity change as a stimulus for miR-467 upregulation in macrophages.

In cultured mouse WT bone marrow-derived macrophages (BMDM), miR-467 was significantly upregulated in response to glucose by 38.7%±28.01 (Fig. 4*E*, p=0.05, n=3).

miR-467 levels were increased in whole BM by 74.13% in mice that were kept on Western diet for 32 weeks (174.3%±42.72 vs. 100.1%±21.95 in chow, p=0.0004) compared to chow-fed mice (Fig. 4*F*).

miR-467 in pancreas and the effects of the antagonist injections

To assess whether the size and the number of pancreatic islets and the insulin production were affected in pancreas of mice injected with the antagonist, sections of pancreas were stained with the anti-insulin antibody and counterstained with hematoxylin (Fig. 5*A*-*C*). The islet area and insulin secretion in the pancreas were unchanged in miR-467 antagonist-injected mice at the end of the experiment.

We have previously reported that miR-467 promotes angiogenesis (5; 6). The potential effect of miR-467 antagonist on vascularization in the pancreas was assessed by immunohistochemistry with anti-vWF and anti-α-actin antibodies, to visualize the markers of endothelial and vascular smooth muscle cells, respectively (Figs. 5*D* and *E*). There was no change in the vascular cell markers in mice injected with the miR-467 antagonist or in response to the Western diet. At the end of the experiment, the levels of a target of miR-467, TSP-1 were not affected by miR-467 antagonist injections or by the diet (Fig. 5*F*).

Mouse pancreatic islets β-cells (βTC-6) were stimulated with high glucose (HG, 30 mM glucose), as described in the Methods, and the levels of miR-467 were measured by QRT-PCR. Glucose-stimulated cells had a 27.7± 4.933% increase in miR-467 expression (Fig. *GH*, p= 0.0284, n=3). In the *in vivo* experiment with mice on the Western diet, the mean value of pancreatic miR-467 was increased two-fold on the

Western diet (208.1%± 173.9vs. 108.6%± 39.04in chow diet), but the difference in the levels at the end of the experiment did not reach statistical significance (Fig. *4H)*.

miR-467 mimic and antagonist regulate production of inflammatory signals by the cultured macrophages

Cultured BMDMs from WT mice were transfected with the miR-467 mimic or 467-antagonist as described in Methods. Expression of *Tnfa*, *Il6*, *Ccl2*, and *Ccl4* were measured by QRT-PCR. The levels of all four cytokines were increased by HG (Figs. 6*A* and *B*). There was no further increase in the levels of *Tnfa*, *Ccl2*, and *Ccl4* in response to overexpression of the miR-467 mimic (Fig. 6*A*). *Il6* was increased by miR-467, but the increase did not reach statistical significance.

Inhibition of miR-467 with the antagonist prevented the upregulation of cytokines in response to HG (Fig. 6*B*).

When cultured BMDM isolated from *Thbs1*$^{-/-}$ mice were transfected with the miR-467 mimic or antagonist, upregulation by high glucose was similar to the cells from the WT mice (Figs. 6*C* and *D*).

Inhibition of miR-467 by the antagonist prevented upregulation of all four cytokines in response to HG (Fig. 6*D*), similar to the WT cells.

TSP-1 knockout eliminates the effects of miR-467 antagonist on blood glucose and insulin levels and IR

To determine whether TSP-1 is a main target of miR-467 in prevention of IR, injections of the miR-467 antagonist were given to *Thbs1*$^{-/-}$ mice on chow and Western diets.

Unlike in WT mice, inhibiting miR-467 in *Thbs1*$^{-/-}$ mice did not result in changes of levels of fasting blood glucose or insulin (Fig. 7*A* and 7*B*), or glucose tolerance and insulin sensitivity (Fig. 7*C* and *D*). Fasting insulin levels were lower than in WT mice (Fig. 1*B* and 7*B*), but were still increased in Western diet-fed mice ($p<0.05$).

Similar to WT mice (Fig. 1), weight was increased by the Western diet. Notably, in the absence of TSP-1, mice injected with the miR-467 antagonist tended to have lower body weights (Fig. 7*E*). Levels of HDL, LDL, cholesterol were upregulated by the Western diet (Fig. 7*F*). All of the indices of lipoprotein metabolism tended to be reduced in mice on the Western diet in response to the miR-467 antagonist.

TSP-1 knockout prevents the accumulation of macrophages in adipose tissue and pancreas of mice injected with the miR-467 antagonist

In *Thbs1*$^{-/-}$ mice, the effect of the miR-467 antagonist injections on the accumulation of macrophages in adipose tissue and pancreas was prevented (Figs. 7*G* and *H*). However, unlike in WT mice where the Western diet increased the accumulation of macrophages in adipose tissue (Fig. 2*A*), in *Thbs1*$^{-/-}$ mice, there was no difference between the accumulation of macrophages in adipose tissue or pancreas of mice on chow and mice on the Western diet (Figs. 7*G* and *H*).

Differential effects of the miR-467 antagonist on plasma levels of inflammatory cytokines

Plasma levels of MCP-1, IL-10, VEGF-A, and CXCL1 were measured in WT and *Thbs1*$^{-/-}$ mice on the chow and the Western diet (Fig. 8). MCP-1, IL-10, and CXCL1 levels were

significantly increased by the Western diet in mice of both genotypes (Fig. 8*A*, B, and C). VEGF-A was not increased by the Western diet (Fig. 8*D*).

The miR-467 antagonist increased the level of MCP-1 in WT mice on the Western diet (Fig. 8*A*, p=0.05) but not in *Thbs1*$^{-/-}$ mice. The antagonist tended to decrease the levels of IL-10 in WT mice on the Western diet (Fig. 8*B*, p=0.06), but this effect was lost in the *Thbs1*$^{-/-}$ mice. There was no effect of the antagonist on CXCL1 or VEGF-A levels (Fig. 8*C* and *D*).

DISCUSSION

miR-467 levels are normally low or undetectable and are rapidly upregulated in response to high glucose (5; 6; 13). As was shown in experiments with miRNA mimics and antagonists, miR-467 regulates angiogenesis (5; 6) and vascular inflammation (8; 14). We hypothesized that physiological functions of this miRNA may be associated with blood glucose handling and may be observed in situations when the regulation of blood glucose levels becomes challenging, e.g., in a model of a diet-induced IR. Inflammation in tissues is associated with IR and often precedes it (10; 15-19). We found that miR-467 prevents IR and macrophage infiltration of metabolically active tissues in response to the Western diet.

Blocking miR-467 with a sequence-specific antagonist caused increases in fasting blood glucose and insulin and IR. Decrease in insulin sensitivity is frequently associated with the weight gain and changes in lipoprotein profile (20) and is often thought to be a direct consequence of the weight gain and changes in the lipoprotein profile. However, the sequence and causality of events in development of IR are still poorly understood (21). When we inhibited miR-467, the development of IR and changes in the blood glucose and insulin levels were uncoupled from the weight gain and impairment of lipoprotein metabolism: in mice injected with miR-467 antagonist, there were no changes in weight or lipoprotein profile on either the chow or the Western diet, demonstrating that IR developed as a direct result of miR-467 inhibition unrelated to the changes in lipid metabolism or weight.

The inhibition of miR-467 increased infiltration of macrophages in the adipose tissue and in the pancreas, suggesting that miR-467 prevents inflammation. The increase in

macrophages infiltration in adipose tissue was associated with the increased IL-6 levels. However, the levels of TNFα, Ccl2, Ccl4, and Il1β were not changed by the antagonist injections in mice on chow diet, and the levels of TNFα and Ccl2 were even reduced in mice on the Western diet injected with the antagonist. These results suggest a specific and complex regulation of inflammatory functions by miR-467.

miR-467 antagonist changed the morphology of the adipocytes: the size of the adipocytes tended to be higher in mice injected with the antagonist. Increased adipocyte size is associated with adipocyte hypoxia, increased inflammation in the adipose tissue, and the development of IR (10; 22).

miR-467 regulates the production of a potent anti-angiogenic protein TSP-1 (5; 13). This regulation appears to be central in regulation of angiogenesis in a mouse cancer model (5; 6). However, a lack of vascular changes in pancreas and adipose tissue in response to the miR-467 antagonist suggested that regulation of vascular remodeling is not the primary function of miR-467 in prevention of IR.

miR-467 was upregulated by high glucose in the cultured macrophage-like cell lines, in the primary bone-marrow-derived macrophages (BMDM). The increased levels of miR-467 coincided with the inhibition of TSP-1 production by these cells, suggesting that macrophages contribute into the regulation of the miR-467-dependent pathways and that the infiltration with macrophages may enhance the significance of the pathway in metabolically active tissues. Upregulation of miR-467 in the bone marrow of hyperglycemic mice (both diet-induced and STZ-induced) further supported our observation of miR-467 upregulation in cultured macrophages.

miR-467 regulated the pro-inflammatory functions of cultured BMDM: the expression of four cytokines, *Tnfa, Il6, Ccl2, and Ccl4*, was upregulated by high glucose, but the increase was prevented by the miR-467 antagonist. The effect of miR-467 inhibition on the cytokine production by cultured BMDM was observed in cells from both the WT and *Thbs1*$^{-/-}$ mice, indicating that TSP-1 is not the mediator of these effects of miR-467. These results suggest other unidentified miR-467 targets and inflammation-related pathways activated by this miRNA.

TSP-1 is an experimentally confirmed target of miR-467 (5; 6; 13) and the central target of miR-467 in regulation of angiogenesis (5; 13). Interestingly, in the diet-induced IR model, we found that the increase in the levels of fasting blood glucose and insulin, the development of IR, and the accumulation of macrophages in adipose tissue were TSP-1-dependent, but the production of cytokines by macrophages was not. These results suggest that the inflammation is regulated by miR-467 through multiple targets. The regulation of additional targets of miR-467 was also suggested by the changes of the metabolic indexes in *Thbs1*$^{-/-}$ mice injected with the antagonist of miR-467: in the absence of TSP-1, the miR-467 antagonist tended to decrease the glucose intolerance, insulin resistance, and also decreased the weights of mice on both diets and the lipoproteins and cholesterol in mice on the Western diet.

In this report, we describe a new physiological role for miR-467: prevention of IR in response to dietary factors inducing inflammation and IR. Our results demonstrated that, by inhibiting the action of miR-467 or of its target TSP-1, one can uncouple IR and lipoprotein metabolism as well as some aspects of inflammation and IR. miR-467 employs multiple targets in regulating the IR, but the prevention of tissue macrophage

infiltration and IR depend on TSP-1 as a target of miR-467. Both miR-467 and TSP-1 may prove to be therapeutic targets to prevent and treat IR. In addition to TSP-1, miR-467 appears to have other unidentified targets that may become useful in controlling the weight and lipid metabolism.

AUTHOR CONTRIBUTIONS

Jasmine Gajeton performed experiments, analyzed experimental data, developed experimental plan, and wrote the manuscript.

Irene Krukovets performed experiments, analyzed experimental data, participated in discussion of the results and preparation of the manuscript.

Revanth Yendamuri performed immunohistochemistry experiments, analyzed experimental data, and participated in discussion of the results and the plan for the manuscript.

Dmitriy Verbovetskiy performed animal experiments, contributed to the discussion of the results and preparation of the manuscript.

Amit Vasanji analyzed the adipocyte size, developed the program and the plan of for these analyses, and participated in the discussion of the result and the manuscript.

Lidiya Sul performed experiments in cultured cells, analyzed experimental data, and participated in discussions of the results and of the manuscript.

Olga Stenina-Adognravi sponsored the project, developed the experimental design, participated in generation of immunohistochemistry data, analyzed experimental data, and prepared the manuscript.

The first author, Jasmine Gajeton, and the corresponding author, Olga Stenina-Adognravi, take full responsibility for the work as a whole, including (if applicable) the study design, access to data, and the decision to submit and publish the manuscript.

ACKNOWLEDGEMENTS

This work was supported by NIH R01CA177771 (O.S.-A.), R01HL117216 (O.S.-A.), and 17PRE33660475 American Heart Association Pre-Doctoral Fellowship (PI: Jasmine Gajeton, Sponsor: O.S.-A.).

FIGURE LEGENDS

Figure 1 – Injections of miR-467 antagonist result in increased glucose and insulin and increased insulin resistance without affecting weight and lipid profile.

Four-week-old male WT mice were fed with chow or Western Diet for 32 weeks, with weekly injections of a control oligo or a 467-antagonist starting at five weeks of age. Data are from end point. *A:* Fasting blood glucose levels were measured with a glucometer. *B*: Fasting insulin levels were measured by ELISA. *C-D*: Time course for the intraperitoneal glucose tolerance test (GTT) and insulin sensitivity test (ITT) were performed. #p<0.05 in chow vs Western diet, control oligo; +p<0.05 in Western-fed control oligo vs 467-antag, ^p<0.05 in chow vs Western diet, 467-antag. *E-F*: Area under the curve is shown for GTT and ITT, respectively. *G*: Weight measured at the end of study. *H*: Lipoproteins measured by HDL and LDL/VLDL quantification kit from serum. n=10 mice/group, *p< 0.05 vs. control oligo, #p<0.05 vs. chow diet.

Figure 2 – Injections of miR-467 antagonist increases macrophage accumulation *in vivo*.

A: Macrophage accumulation in adipose tissue was determined by anti-MOMA-2 staining. Positive staining was normalized to mean adipocyte area for adipose tissue since adipocyte sizes were changed between groups. Representative images of staining are shown. Scale bars at 100μM. n=10 mice/group. *B*: Macrophage accumulation in pancreas sections was determined by anti-CD68 staining. Data are normalized to the chow control average % staining. Representative images of staining are shown. Scale bars at 100μM. n=10 mice/group. *C*: Expression of pro-inflammatory markers (*Il6, Tnfa*, *Ccl2*, *Ccl4* and *Il1b*) were assessed in WT whole adipose tissue by

QRT-PCR and normalized to β–actin in mice on chow or Western and injected with the control oligo or the antagonist. n=10 mice/group. *p< 0.05 compared to control oligo, #p<0.05 compared to chow diet. *D*: Whole blood collected at end point was analyzed on a hematology analyzer to determine circulating numbers of monocytes and WBCs in WT (*E*) mice or *Thbs1*$^{-/-}$ mice (*F*). #p<0.05 compared to chow diet.

Figure 3 – miR-467 in adipose tissue and the effects of the antagonist injections.

A: Expression of miR-467 after a 3 hr HG stimulation in cultured mouse fibroblasts (3T3-L1) differentiated into adipocytes was measured by QRT-PCR and normalized to β-actin. n=3 independent replicates. Representative phase contrast image of Oil Red O Staining of 3T3-L1 cells at day 7 post-differentiation. 20x magnification. *B*: Expression of miR-467 in WT C57/BL6 mouse adipose tissue on chow or Western diet for 32 weeks. n=10 mice/group. *C/D*: Mean adipocyte area and perimeter were quantified from H&E-stained sections of adipose tissue. *E*: Quantification of the % positive staining with an anti-TSP-1 antibody. *F*: Quantification of blue color density from Masson's trichrome staining. #p<0.05 vs chow diet.

Figure 4– High glucose upregulates miR-467 in macrophages.

A/*C*: Expression of miR-467 after 3 hours of glucose stimulation in cultured mouse macrophages (RAW 264.7) and differentiated human monocyte (THP-1) cell lines was measured by QRT-PCR and normalized to β-actin, n=3 independent replicates. *B*/*D*: TSP-1 secretion was assessed in cell supernatants after 24 hrs of glucose stimulation by Western Blot. Quantification of densitometry is shown and relative to the control, n=3 independent replicates. *E*: Expression of miR-467 after 6 hours of glucose stimulation in cultured WT BMDM. Data are relative to LG ctrl samples, n=3 independent replicates. *F*:

Expression of miR-467 in whole bone marrow from WT mice on chow or Western diet for 32 weeks, n=10 mice/group.

Figure 5 – miR-467 in pancreas and the effects of the antagonist injections

A: Total insulin staining was quantified as % positive insulin staining multiplied by the real intensity of each sample. *B*: Sections of pancreas were stained for insulin and counterstained with hematoxylin. Islet area was quantified as % positive insulin staining over the total area per 100 pixels. *C*: Representative staining is pictured at 20X magnification, scale bars at 100μM. Quantification of positive staining using an anti-vWF, anti-α-actin, or anti-TSP-1 antibody, (*D-F),* respectively, in pancreas sections. *G*: Expression of miR-467 after glucose stimulation in a cultured mouse β cell line (βTC6) was measured by QRT-PCR and normalized to β-actin. n=3 independent replicates. LG: low glucose control (5 mM D-glucose). HG: high glucose stimulated (30 mM D-glucose). *H*: Expression of miR-467 in C57/BL6 WT mouse pancreas on chow or Western diet for 32 weeks. n=10 mice/group.

Figure 6 – miR-467 blocks pro-inflammatory functions of cultured macrophages.

A: Expression of pro-inflammatory markers (*Tnfa*, *Il6*, *Ccl2*, and *Ccl4*) were assessed in transfected BMDM from WT (*A-B*) or *Thbs1*$^{-/-}$ (*C-D*) mice 6 hours post glucose stimulation by QRT-PCR and normalized to β–actin. Data are relative to the LG control stimulated samples per transfection, n=3 independent replicates.

Figure 7 – TSP-1 is a major target of miR-467 in affecting inflammation and insulin resistance in mice on a long-term Western Diet.

Four-week-old male *Thbs1*$^{-/-}$ mice were fed with chow or Western Diet for 32 weeks, with weekly injections of a control oligo or a 467-antagonist starting at five weeks of

age. Data are from end point. *A:* Fasting blood glucose levels were measured with a glucometer. *B*: Fasting plasma insulin levels were measured by ELISA. *C-D*: Intraperitoneal glucose tolerance test (GTT) and insulin sensitivity test (ITT) were performed. Area under the curve is shown. *E*: Weight measured at the end of study. *F*: Lipoproteins measured by HDL and LDL/VLDL quantification kit from serum. *G*: Macrophage accumulation in adipose tissue was determined by anti-MOMA-2 staining. Positive staining was normalized to mean adipocyte area. *H*: Macrophage accumulation in pancreas sections was determined by anti-CD68 staining. Data are normalized to the chow control average % staining. n=10 mice/group. #p<0.05 compared to chow diet.

Figure 8 – Differential effects of the miR-467 antagonist on plasma levels of inflammatory cytokines.

A-D: Plasma from WT or *Thbs1*$^{-/-}$ mice, collected at 32 weeks, were assayed by U-plex for circulating MCP-1, IL-10, CXCL1 and VEGF-A. #p<0.05 vs chow diet.

REFERENCES

1. Lackey DE, Olefsky JM: Regulation of metabolism by the innate immune system. Nat Rev Endocrinol 2016;12:15-28

2. Memetimin H, Li D, Tan K, Zhou C, Liang Y, Wu Y, Wang S: Myeloid Specific Deletion of Thrombospondin 1 Protects Against Inflammation and Insulin Resistance in Long-term Diet-induced Obese Male Mice. Am J Physiol Endocrinol Metab 2018;

3. Maimaitiyiming H, Clemons K, Zhou Q, Norman H, Wang S: Thrombospondin1 deficiency attenuates obesity-associated microvascular complications in ApoE-/- mice. PLoS One 2015;10:e0121403

4. Li Y, Tong X, Rumala C, Clemons K, Wang S: Thrombospondin1 deficiency reduces obesity-associated inflammation and improves insulin sensitivity in a diet-induced obese mouse model. PLoS One 2011;6:e26656

5. Bhattacharyya S, Sul K, Krukovets I, Nestor C, Li J, Adognravi OS: Novel tissue-specific mechanism of regulation of angiogenesis and cancer growth in response to hyperglycemia. J Am Heart Assoc 2012;1:e005967

6. Krukovets I, Legerski M, Sul P, Stenina-Adognravi O: Inhibition of hyperglycemia-induced angiogenesis and breast cancer tumor growth by systemic injection of microRNA-467 antagonist. FASEB J 2015;

7. Tian GP, Chen WJ, He PP, Tang SL, Zhao GJ, Lv YC, Ouyang XP, Yin K, Wang PP, Cheng H, Chen Y, Huang SL, Fu Y, Zhang DW, Yin WD, Tang CK: MicroRNA-467b targets LPL gene in RAW 264.7 macrophages and attenuates lipid accumulation and proinflammatory cytokine secretion. Biochimie 2012;94:2749-2755

8. Tian GP, Tang YY, He PP, Lv YC, Ouyang XP, Zhao GJ, Tang SL, Wu JF, Wang JL, Peng J, Zhang M, Li Y, Cayabyab FS, Zheng XL, Zhang DW, Yin WD, Tang CK: The effects of miR-467b on lipoprotein lipase (LPL) expression, pro-inflammatory cytokine, lipid levels and atherosclerotic lesions in apolipoprotein E knockout mice. Biochem Biophys Res Commun 2014;443:428-434

9. Amend SR, Valkenburg KC, Pienta KJ: Murine Hind Limb Long Bone Dissection and Bone Marrow Isolation. J Vis Exp 2016;

10. Sun K, Kusminski CM, Scherer PE: Adipose tissue remodeling and obesity. J Clin Invest 2011;121:2094-2101

11. Scherer PE: The many secret lives of adipocytes: implications for diabetes. Diabetologia 2019;62:223-232

12. Crewe C, An YA, Scherer PE: The ominous triad of adipose tissue dysfunction: inflammation, fibrosis, and impaired angiogenesis. J Clin Invest 2017;127:74-82

13. Bhattacharyya S, Marinic TE, Krukovets I, Hoppe G, Stenina OI: Cell type-specific post-transcriptional regulation of production of the potent antiangiogenic and proatherogenic protein thrombospondin-1 by high glucose. J Biol Chem 2008;283:5699-5707

14. Guan XM, Li YX, Xin H, Li J, Zhao ZG, Wang YW, Wang HF: Effect of miR-467b on atherosclerosis of rats. Asian Pac J Trop Med 2016;9:298-301

15. Xu H, Barnes GT, Yang Q, Tan G, Yang D, Chou CJ, Sole J, Nichols A, Ross JS, Tartaglia LA, Chen H: Chronic inflammation in fat plays a crucial role in the development of obesity-related insulin resistance. J Clin Invest 2003;112:1821-1830

16. Florez JC: Newly identified loci highlight beta cell dysfunction as a key cause of type 2 diabetes: where are the insulin resistance genes? Diabetologia 2008;51:1100-1110

17. McCarthy MI: Genomics, type 2 diabetes, and obesity. N Engl J Med 2010;363:2339-2350

18. Petrie JR, Adler A, Vella S: What to add in with metformin in type 2 diabetes? QJM 2011;104:185-192

19. Voight BF, Scott LJ, Steinthorsdottir V, Morris AP, Dina C, Welch RP, Zeggini E, Huth C, Aulchenko YS, Thorleifsson G, McCulloch LJ, Ferreira T, Grallert H, Amin N, Wu G, Willer CJ, Raychaudhuri S, McCarroll SA, Langenberg C, Hofmann OM, Dupuis J, Qi L, Segre AV, van Hoek M, Navarro P, Ardlie K, Balkau B, Benediktsson R, Bennett AJ, Blagieva R, Boerwinkle E, Bonnycastle LL, Bengtsson Bostrom K, Bravenboer B, Bumpstead S, Burtt NP, Charpentier G, Chines PS, Cornelis M, Couper DJ, Crawford G, Doney AS, Elliott KS, Elliott AL, Erdos MR, Fox CS, Franklin CS, Ganser M, Gieger C, Grarup N, Green T, Griffin S, Groves CJ, Guiducci C, Hadjadj S, Hassanali N, Herder C, Isomaa B, Jackson AU, Johnson PR, Jorgensen T, Kao WH, Klopp N, Kong A, Kraft P, Kuusisto J, Lauritzen T, Li M, Lieverse A, Lindgren CM, Lyssenko V, Marre M, Meitinger T, Midthjell K, Morken MA, Narisu N, Nilsson P, Owen KR, Payne F, Perry JR, Petersen AK, Platou C, Proenca C, Prokopenko I, Rathmann W, Rayner NW, Robertson NR, Rocheleau G, Roden M, Sampson MJ, Saxena R, Shields BM, Shrader P, Sigurdsson G, Sparso T, Strassburger K, Stringham HM, Sun Q, Swift AJ, Thorand B, Tichet J, Tuomi T, van Dam RM, van Haeften TW, van Herpt T, van Vliet-Ostaptchouk JV, Walters GB, Weedon MN, Wijmenga C, Witteman J, Bergman RN, Cauchi S, Collins FS, Gloyn AL, Gyllensten U, Hansen T, Hide WA, Hitman GA,

Hofman A, Hunter DJ, Hveem K, Laakso M, Mohlke KL, Morris AD, Palmer CN, Pramstaller PP, Rudan I, Sijbrands E, Stein LD, Tuomilehto J, Uitterlinden A, Walker M, Wareham NJ, Watanabe RM, Abecasis GR, Boehm BO, Campbell H, Daly MJ, Hattersley AT, Hu FB, Meigs JB, Pankow JS, Pedersen O, Wichmann HE, Barroso I, Florez JC, Frayling TM, Groop L, Sladek R, Thorsteinsdottir U, Wilson JF, Illig T, Froguel P, van Duijn CM, Stefansson K, Altshuler D, Boehnke M, McCarthy MI, investigators M, Consortium G: Twelve type 2 diabetes susceptibility loci identified through large-scale association analysis. Nat Genet 2010;42:579-589

20. Zheng S, Xu H, Zhou H, Ren X, Han T, Chen Y, Qiu H, Wu P, Zheng J, Wang L, Liu W, Hu Y: Associations of lipid profiles with insulin resistance and beta cell function in adults with normal glucose tolerance and different categories of impaired glucose regulation. PLoS One 2017;12:e0172221

21. Petersen MC, Shulman GI: Mechanisms of Insulin Action and Insulin Resistance. Physiol Rev 2018;98:2133-2223

22. Choe SS, Huh JY, Hwang IJ, Kim JI, Kim JB: Adipose Tissue Remodeling: Its Role in Energy Metabolism and Metabolic Disorders. Front Endocrinol (Lausanne) 2016;7:30

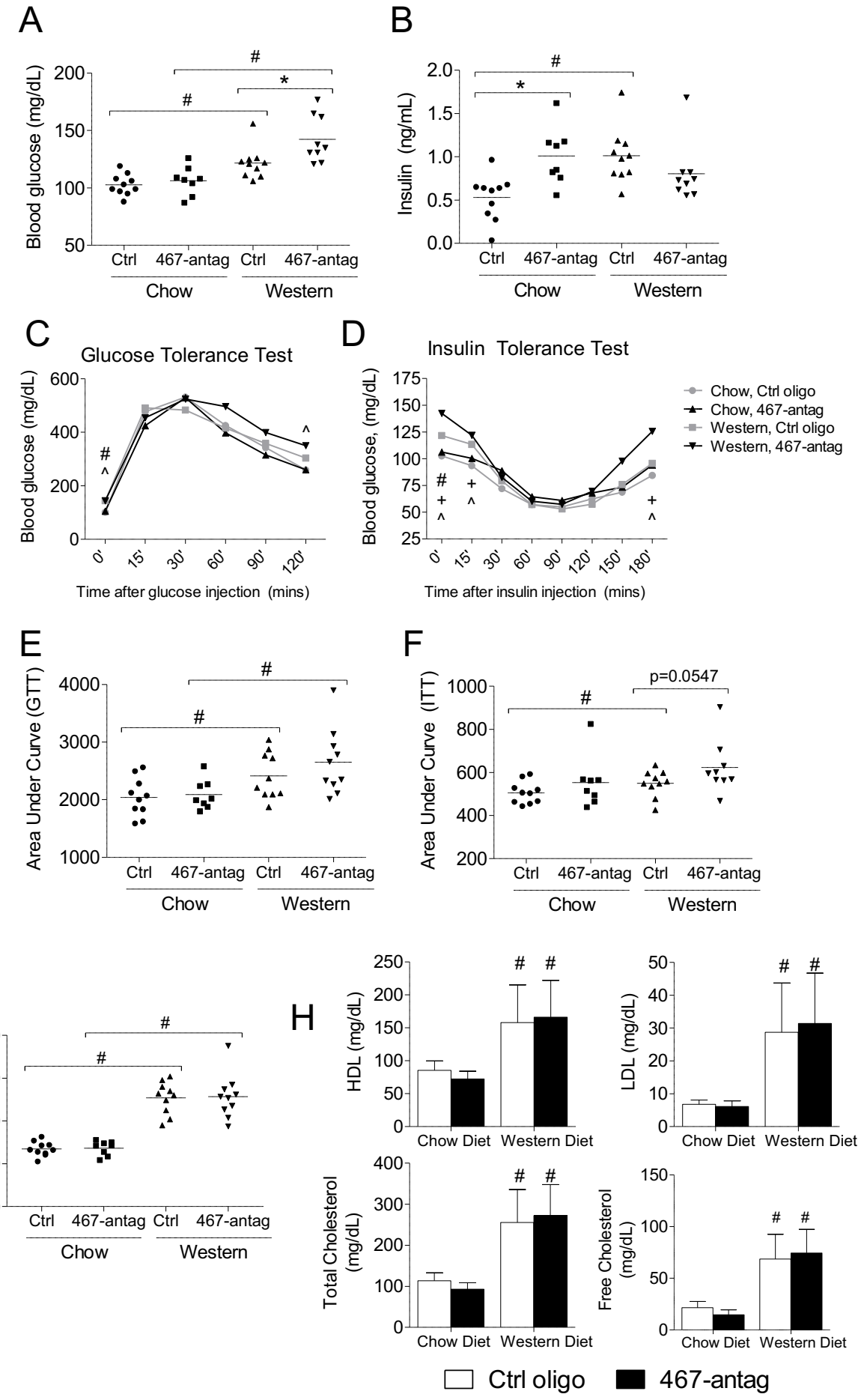

A

Adipose Tissue

MOMA-2 Staining (% per 100 pixels)

Ctrl 467-antag Ctrl 467-antag

Chow Western

Control oligo 467-antagonist

Western Diet Chow Diet

B

Pancreas

CD68 Staining (%)

Ctrl 467-antag Ctrl 467-antag

Chow Western

Control oligo 467-antagonist

Western Diet Chow Diet

C

Adipose Tissue

Chow Ctrl oligo
Chow 467-antag
Western Ctrl oligo
Western 467-antag

Relative expression

p=0.0929

p=0.0827

Il6 *Tnfa* *Ccl2* *Ccl4* *Il1b*

D

Monocytes ($x10^3$ cells/µL)

Monocytes (%)

WBC ($x10^3$ cells/µL)

Ctrl 467-antag Ctrl 467-antag

Chow Western

E

Thbs1$^{-/-}$ Mice

Monocytes ($x10^3$ cells/uL)

Monocytes (%)

WBC ($x10^3$ cells/µL)

Ctrl 467-antag Ctrl 467-antag

Chow Western

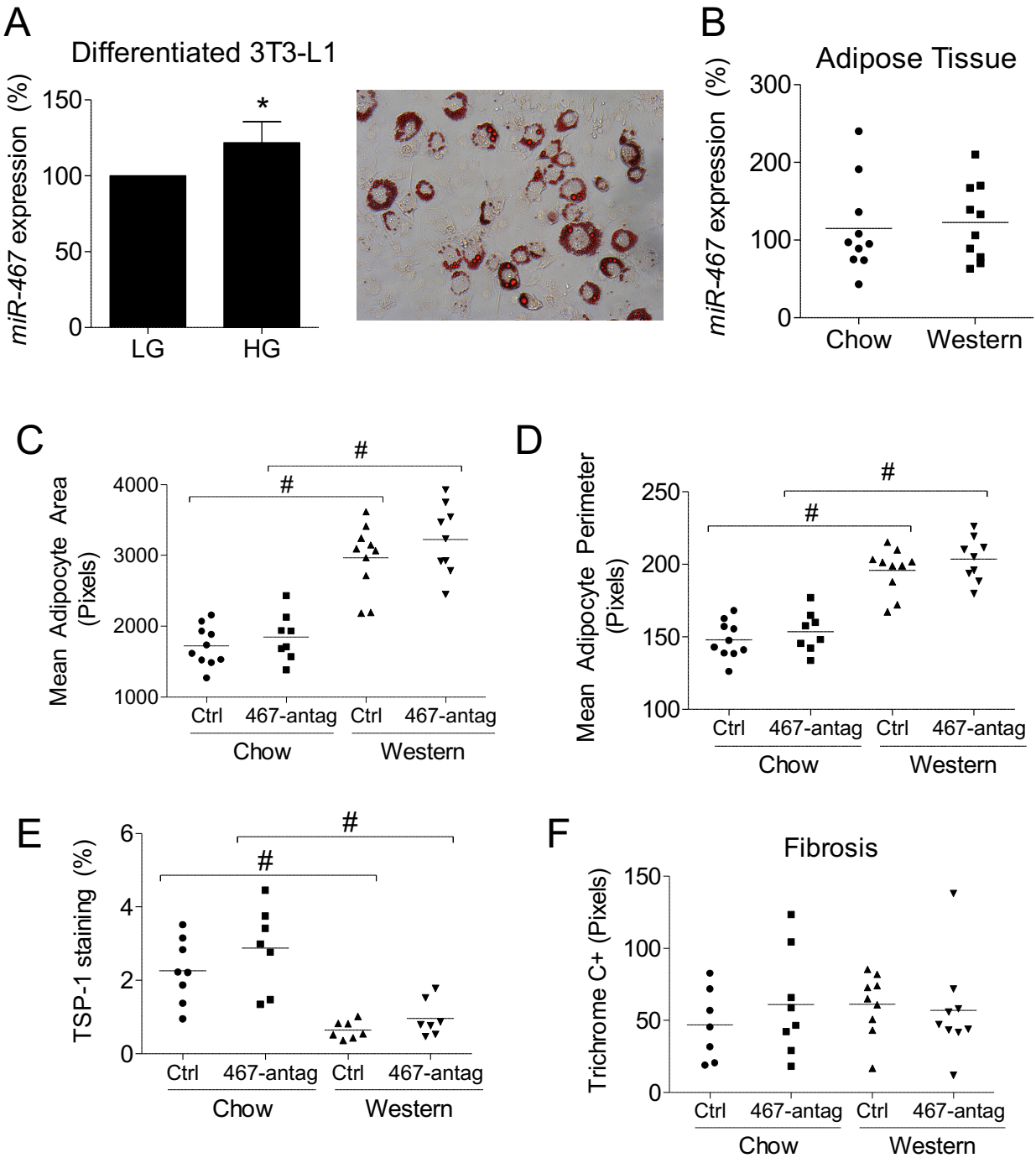

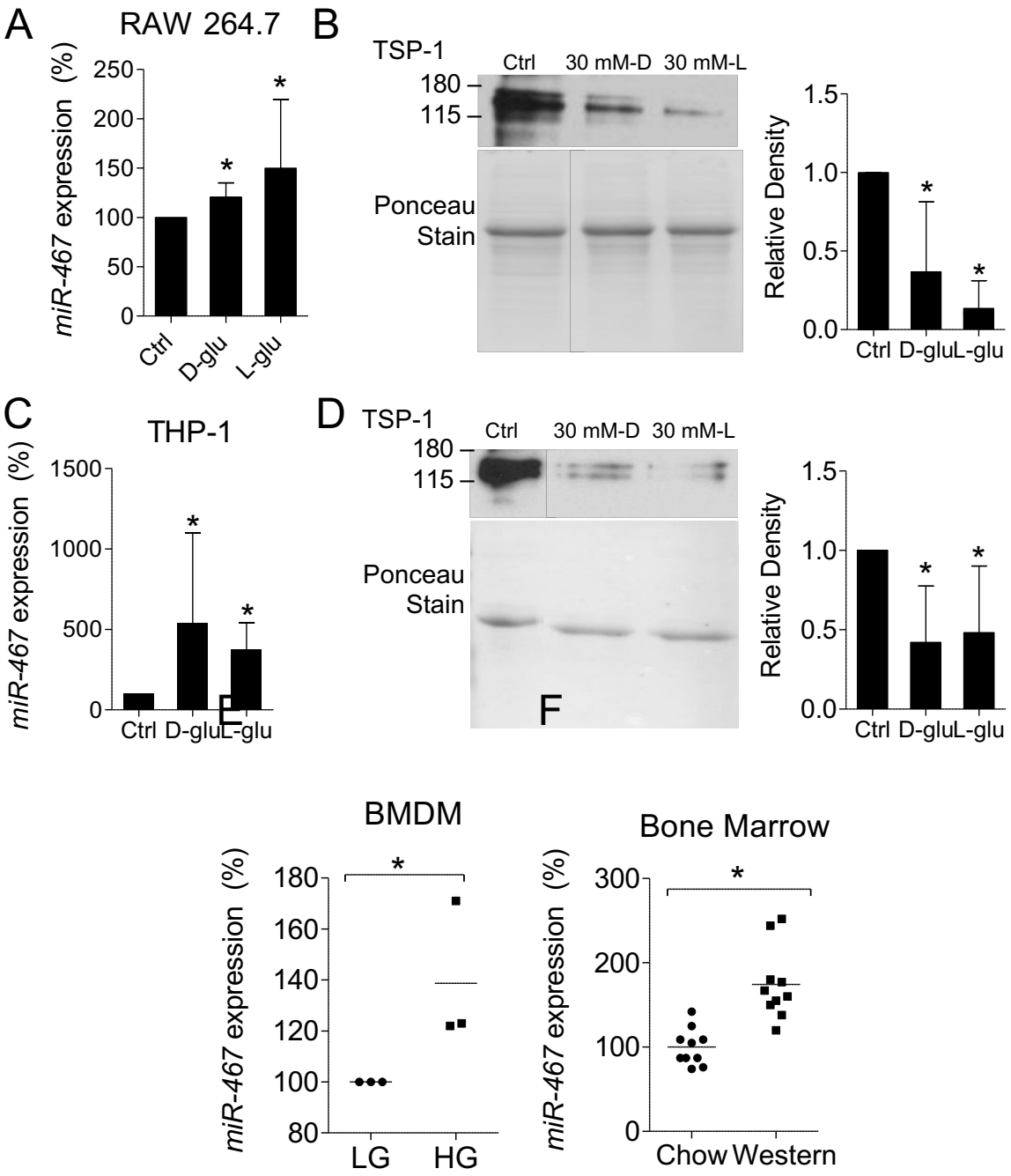

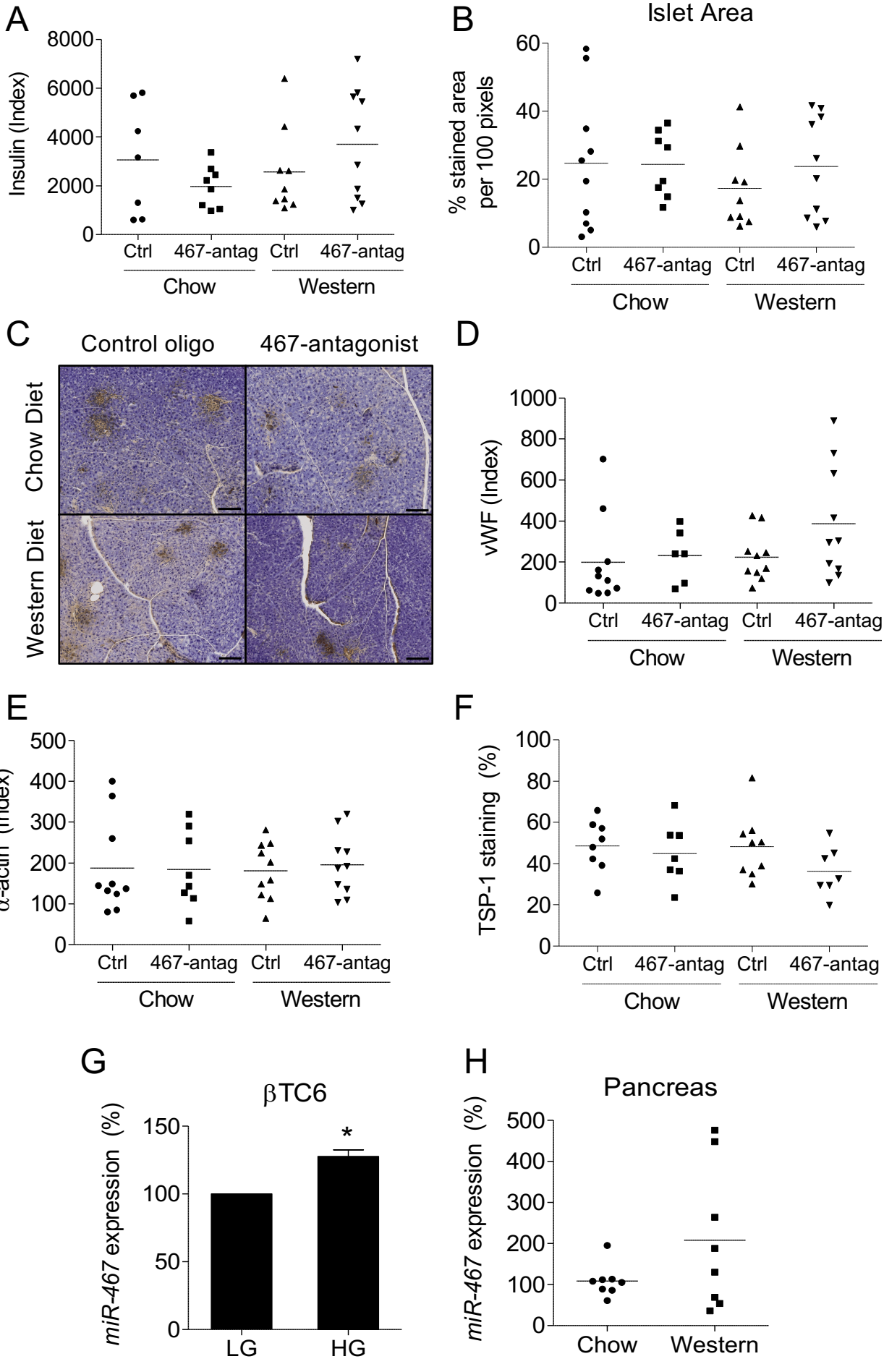

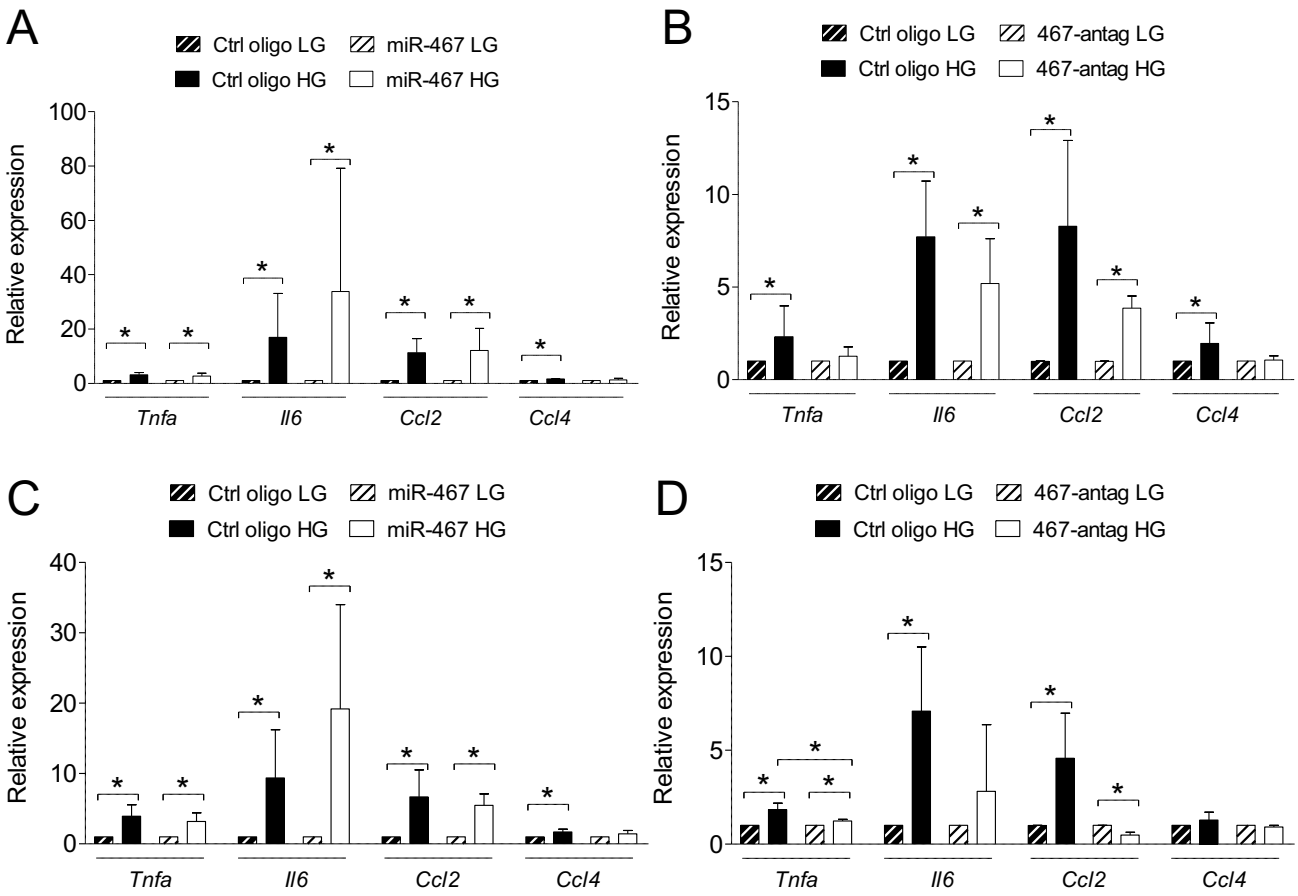

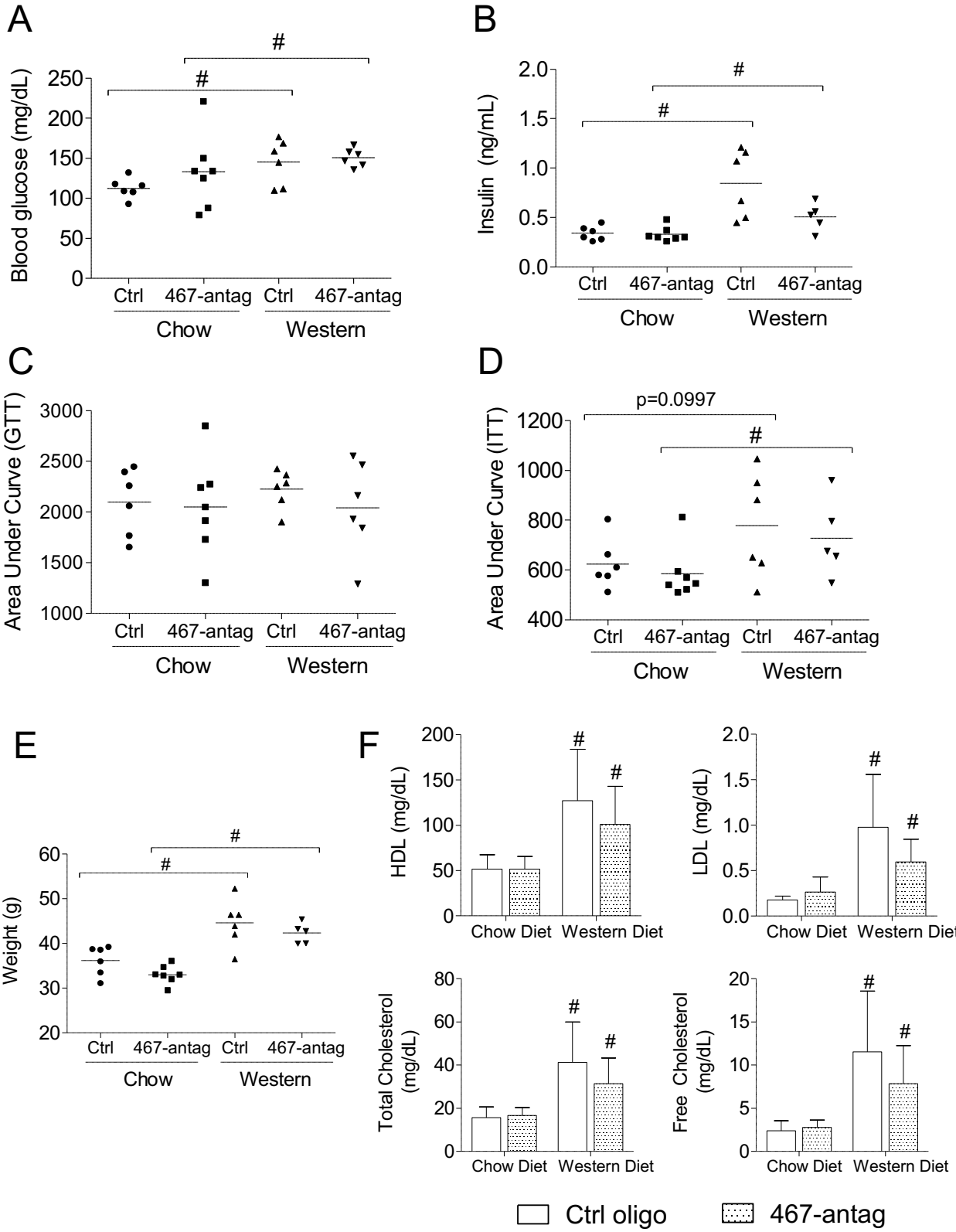

A

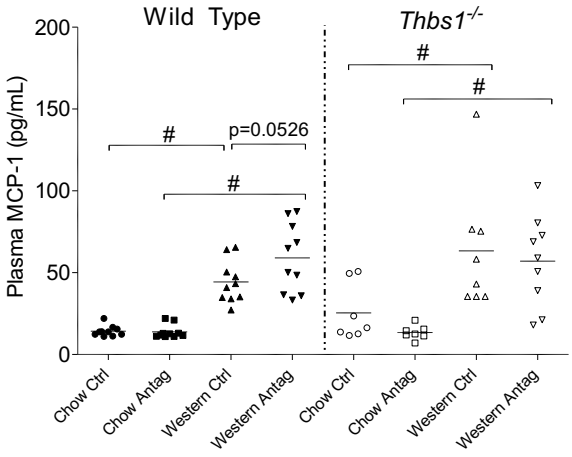

B

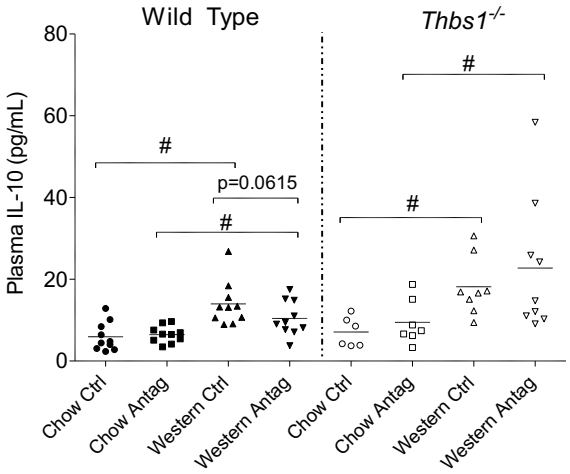

C

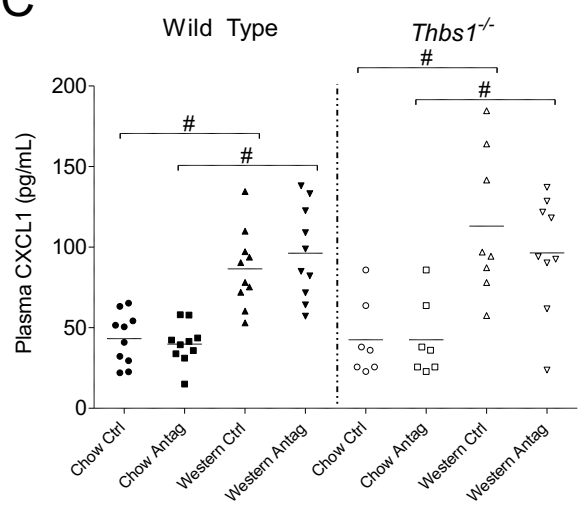

D